

1 Responses to referees' comments and listed changes

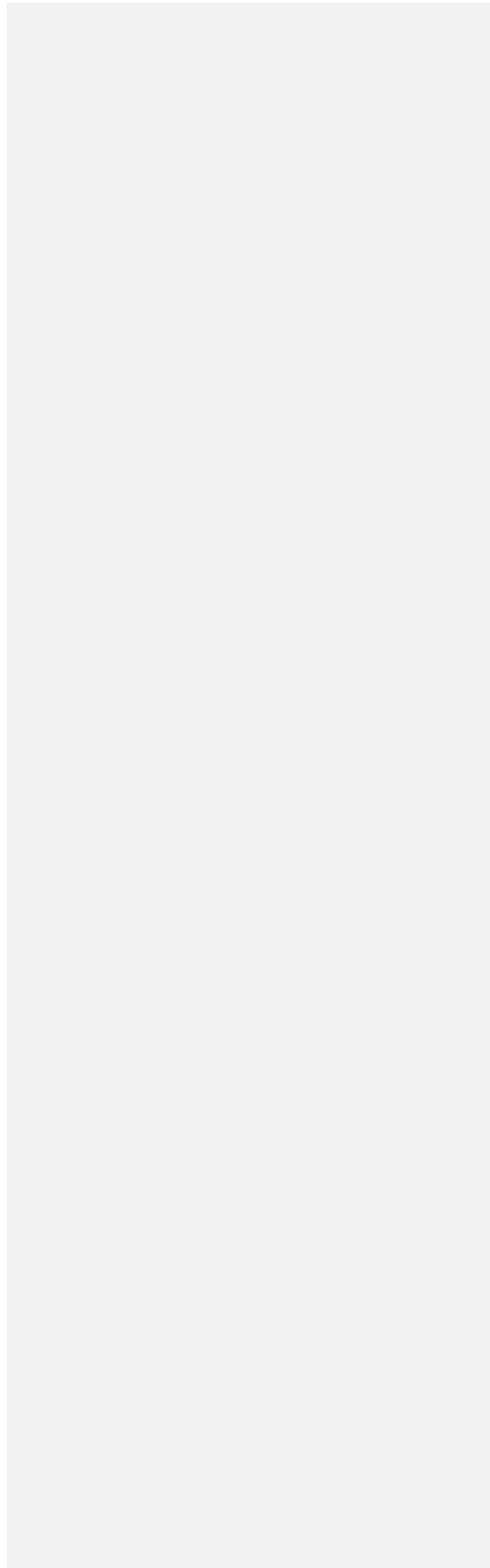
2

Referee 1	Response and changes made
<p><b>The paper is clear, scientifically sound, and well written. It represents an important study in the field of biomass and carbon forest monitoring, as few multitemporal lidar studies are available and none in the Mediterranean ecosystem under analysis. The methods are sound and the discussion is interesting. Minor scientific questions are posed below.</b></p>	
<p>Line 118-121: How did you measure DBH, crowns etc. for shrubs? The list of what measured seems as better suited for trees not shrubs. Same applies for biomass calculation (line 122 to 130). In Med. Woodlands shrubs below and among trees can be consistent, and it would be interesting to understand if you measure them (and how) and how shrubs presence influence your study</p>	<p>We measure shrubs and trees setting the DBH threshold to 7.5. We considered that smaller sizes do not significantly contribute to plot-level biomass: this is now explained with appropriate reference (Stephenson <i>et al</i> 2014, Nature) in lines 122-4.</p>
<p>Line 152: The amount of ground truth plots for developing the lidar biomass map is quite limited. How this influenced the goodness of estimates (and the low coeff. Of determination you obtained). Did you perform additional validation of the lidar modelled AGB i.e with leave one out or similar method? May the low R2 be responsible for the large st. dev. of your AGB change map? Which are the reference values (R2) for lidar based AGB estimation in Mediterranean woodlands? The analysis of this issues can improve the study.</p>	<p>We acknowledge that the number of ground truth plots is low, and have added some text to:</p> <ul style="list-style-type: none"> <li>- emphasise the importance of the validation of the lidar modelled AGB using independent datasets (lines 178-79), and</li> <li>- suggest that the results of this validation indicate that the sample size was sufficient statistically to obtain the estimated parameters of our model.</li> </ul> <p>We also compare the coefficient of determination of the AGB model (0.53) with a reference value from the region (0.67) (lines 299-302).</p> <p>Despite these additions to the revised version we didn't consider that the additional analysis suggested, because we are confident that the results will remain the same and anyway the data is enough to support</p>

	the results and conclusions of our analyses.
Line 63: airborne lidar cannot support large scale applications, is not cost-effective. Line 70: to lidar in? Line 77: I would add that multitemporal lidar acquisitions are still too expensive tool	We agree that the costs of lidar are still high, and this point has now been emphasised in the discussion of making lidar operational in the future for better spatial and temporal coverage (lines 76, 344). We mention future space lidar capability as being an exciting development in this regard. However, it cannot be disputed that national level lidar applications are emerging, so the 'large-scale' use is still referred to.
<b>Referee 2</b>	
<b>Very good and inspiring paper that I really enjoyed reading. It is a step ahead in the process of operationalising the use of LiDAR for quantifying AGB and Carbon fluxes. The authors use a study in central Spain with data from archive and ground data collection as an example of other research work worldwide. I liked the use of cores and dendrochronology applied to the estimation of carbon. It opens my mind personally for a lot of possible applications using the same data</b>	
Please, include a couple of sentences describing how cores are being extracted (e.g. just one core, two cores in N-S, E-W, at dbh level, at mid point from ground to base of canopy .etc). I assume most of the readers, including myself, may not get access to the reference you mentioned that supposedly describes this process	Further information has been inserted, as follows: One core was extracted from each selected tree at a height of 1.3 m off the ground. Following a size-stratified random sampling approach, 12 trees per plot were cored in monocultures and 6 trees per species were cored in mixtures (lines 196-200)
Please specify whether altitude is referred to above ground or above sea level	Comment refers to flying altitude in Table 1. It is now clarified that this is above sea level (asl)
Page 14750, I think the authors should be talking more openly about Return Periods for extreme events in years rather than probabilities. I believe the first concept	Agreed, and return rates are now referred to in lines 38, 284 and 384-5.

<p>is better understood and transmit a far more powerful message</p>	
<p>The probabilities they used for their predictions are perhaps not very realistic, as the authors noticed at the end of the paper. They only contemplate fire events every 100, 250 and 500 years, whereas in Cataluña these returns periods are far shorter</p>	<p>The rates we used did seem conservative but were based on the only two sources of information that we found for the Guadalajara region: (Ministerio de Agricultura, 2002, 2012) and (Purves et al., 2007).</p>
<p>I think the size of the plots (30x30m) is big enough for calibrating the system. I do not believe they may introduce important errors. In our experiments with plantation forests, 30 meters is precisely the point where accuracy levels of.</p>	<p>This is encouraging, and we have made this point in line 328-329.</p>

3  
4  
5



## 6 **Modelling above-ground carbon dynamics using multi-temporal airborne** 7 **lidar: insights from a Mediterranean woodland**

8 William Simonson<sup>1,2\*</sup>, Paloma Ruiz-Benito<sup>2,3</sup>Benito<sup>3,4</sup>, Fernando Valladares<sup>4,5</sup>Valladares<sup>5,6</sup>,  
9 David Coomes<sup>1</sup>

11 <sup>1</sup> Forest Ecology and Conservation Group, Department of Plant Sciences, University of Cambridge, Cambridge  
12 CB2 3EA, UK

13 <sup>2</sup> [United Nations Environment Programme World Conservation Monitoring Centre, 219 Huntingdon Road,](#)  
14 [Cambridge CB3 0DL, UK](#)

15 <sup>3</sup> Biological and Environmental Sciences, School of Natural Sciences, University of Stirling, Stirling, FK9 4LA,  
16 UK

17 <sup>4</sup> Forest Ecology and Restoration Group, Department of Life Sciences, University of Alcalá, Science Building,  
18 Campus Universitario, 28871 Alcalá de Henares, Madrid

19 <sup>45</sup> Museo Nacional de Ciencias Naturales, CSIC, Serrano 115 dpdo, E28006 Madrid, Spain

20 <sup>56</sup> Departamento de Ciencias, Universidad Rey Juan Carlos, Mostoles, Madrid, Spain.

22 \*Correspondence email for proofs: wds10@cam.ac.uk

### 24 **Abstract**

25 Woodlands represent highly significant carbon sinks globally, though could lose this function  
26 under future climatic change. Effective large-scale monitoring of these woodlands has a  
27 critical role to play in mitigating for, and adapting to, climate change. Mediterranean  
28 woodlands have low carbon densities, but represent important global carbon stocks due to  
29 their extensiveness and are particularly vulnerable because the region is predicted to become  
30 much hotter and drier over the coming century. -Airborne lidar is already recognized as an  
31 excellent approach for high-fidelity carbon mapping, but few studies have used multi-  
32 temporal lidar surveys to measure carbon fluxes in forests and none have worked with  
33 Mediterranean woodlands. We use a multi-temporal (five year interval) airborne lidar dataset  
34 for a region of central Spain to estimate above-ground biomass (AGB) and carbon dynamics  
35 in typical mixed broadleaved/coniferous Mediterranean woodlands. Field calibration of the  
36 lidar data enabled the generation of grid-based maps of AGB for 2006 and 2011, and the  
37 resulting AGB change ~~were~~was estimated. There was a close agreement between the lidar-  
38 based AGB growth estimate (1.22 Mg/ha/yr) and those derived from two independent  
39 sources: the Spanish National Forest Inventory, and a tree-ring based analysis (1.19 and 1.13  
40 Mg/ha/yr, respectively). We parameterised a simple simulator of forest dynamics using the  
41 lidar carbon flux measurements, and used it to explore four scenarios of fire occurrence.  
42 Under undisturbed conditions (no fire ~~occurrence~~) an accelerating accumulation of biomass  
43 and carbon is evident over the next 100 years with an average carbon sequestration rate of  
44 1.95 Mg C/ha/year. This rate reduces by almost a third when fire probability is increased to  
45 0.01, (fire return rate of 100 years), as has been predicted under climate change. Our work  
46 shows the power of multi-temporal lidar surveying to map woodland carbon fluxes and

Formatted: Space Before: 0 pt, After: 6 pt

Formatted: Left

47 provide parameters for carbon dynamics models. Space deployment of lidar instruments in the  
48 near future could open the way for rolling out wide-scale forest carbon stock monitoring to  
49 inform management and governance responses to future environmental change.

50

51 Keywords: forest, woodland, lidar, laser scanning, carbon accounting

52

53

## 54 1. Introduction

55 The world's forests are currently acting as an important carbon sink, in 2000–2007 taking up  
56  $2.3 \pm 0.5$  PgC each year compared with anthropogenic emissions of  $8.7 \pm 0.8$  PgC (Pan et al.,  
57 2011). For this reason, the international community recognises that forest protection could  
58 play a significant role in climate change abatement and that the feedback between climate and  
59 the terrestrial carbon cycle will be a key determinant of the dynamics of the Earth System  
60 (Purves et al., 2007). However, there is major uncertainty over forest responses to  
61 anthropogenic global change, and concerns that the world's forests may switch from being a  
62 sink to a source within the next few decades (Nabuurs et al., 2013; Ruiz-Benito et al., 2014b),  
63 through gradual effects on regeneration, growth and mortality, as well as climate-change  
64 related disturbance (Frank et al., 2015). For instance, severe droughts in many parts of the  
65 world are causing rapid change, killing trees directly through heat-stress and indirectly by fire  
66 (Allen et al., 2010). Disturbance events can cause major perturbations to regional carbon  
67 fluxes (Chambers et al., 2013; Vanderwel et al., 2013). A major goal in biogeosciences,  
68 therefore, is to improve understanding of the terrestrial vegetation carbon cycle to enable  
69 better constrained projections (Smith et al., 2012).

70 In this context, remote sensing methods for modelling above ground storage of carbon in  
71 biomass have received much recent attention, with airborne light detection and ranging (lidar)  
72 showing the most potential for accurate and large-scale applications. Lidar metrics of canopy  
73 structure are highly correlated with field-based estimates of above-ground biomass (AGB)  
74 and carbon (AGC) (Drake et al., 2003; Lefsky et al., 2002). With such relationships being  
75 repeatedly demonstrated, it has been possible to develop a conceptual and technical approach  
76 linking plot-based carbon density estimates with lidar top-canopy heights using regional  
77 inputs on basal area and wood density (Asner and Mascaro, 2014). With the increasing  
78 availability of multi-temporal (repeat survey) lidar datasets, including some of national  
79 coverage, a few researchers have started to use lidar in large-scale studies of vegetation  
80 productivity and carbon dynamics (Englhart et al., 2013; Hudak et al., 2012) as well as forest  
81 disturbance and gap dynamics (Blackburn et al., 2014; Kellner and Asner, 2014; Vepakomma  
82 et al., 2008, 2010, 2011). As such, and despite its high costs, lidar is transitioning from  
83 research to practical application, notably in supporting baseline surveys and monitoring of  
84 carbon stocks required for the implementation of the REDD+ mechanism (Reducing  
85 Emissions from Deforestation and Forest Degradation) (Asner et al., 2013). However,

Formatted: Left

86 monitoring carbon fluxes using multi-temporal lidar is technically challenging because  
87 instrument and flight specifications vary over time (Réjou-Méchain et al., ~~2014~~2015).

Field Code Changed

88 The applications of airborne lidar for modelling AGB and AGC have largely been tested in  
89 cool temperate and tropical forest systems (see Zolkos et al., 2013). Less attention has been  
90 given to the effectiveness of the technology for the modelling of biomass and carbon in sub-  
91 tropical and Mediterranean climate zones dominated by dry woodlands. These woodlands  
92 have lower carbon densities, but represent important global carbon stocks due to their  
93 extensiveness and also vulnerability in the face of climate change (Ruiz-Benito et al., 2014b).  
94 As elsewhere in Europe, carbon stocks in such woodlands have been increasing in recent  
95 decades (Nabuurs et al., 2003, 2010; Vayreda et al., 2012), as woodland management for  
96 charcoal and timber has declined in profitability. However, with Earth System models  
97 predicting some of the most severe warming and drying trends of anywhere in the world  
98 (Giorgi and Lionello, 2008; Valladares et al., 2014), abrupt shifts in increasing fire frequency  
99 and intensity may reverse such trends across the Mediterranean region (Pausas et al., 2008).  
100 Lidar has been used to measure carbon stocks in some Mediterranean woodlands (García et  
101 al., 2010) but, to our knowledge, not for measuring carbon dynamics.

102 In this study we demonstrate the potential to build a patchwork dynamics simulator for the  
103 biomass and carbon dynamics in Mediterranean woodlands based on multi-temporal lidar data  
104 (Fig. 1). Our aim is to model the direction and rate of landscape-scale AGC change for mixed  
105 oak-pine woodland in central Spain. We first calibrate a lidar top-of-canopy height model  
106 using selective ground-based estimations of tree- and plot-level biomass. The lidar-based  
107 AGB growth models are then validated using two independent datasets: the Spanish National  
108 Forest Inventory (SFI) and tree-ring measurements, before parameterising a simulation model  
109 to explore the dynamics of carbon change over a 100 year period. In doing so, we explore  
110 sensitivity of the long-term carbon sequestration potential of the regional landscape to  
111 increasing forest fire frequency, as is to be expected under future climate change.

## 112 2. Methods

### 114 2.1 Study area

115 Alto Tajo (40° 47' N, 2° 14' W) is a Natural Park (32,375 ha) situated in the Guadalajara  
116 province of Central Spain. The dominant woody vegetation is Mediterranean mixed  
117 woodland, comprising *Pinus sylvestris*, *P. nigra*, *Quercus faginea*, *Q. ilex*, *Juniperus*  
118 *oxycedrus* and *J. thurifera*. The region has a complex topography ranging from 960 to 1400 m  
119 a.s.l. The mean annual temperature here is 10.2 °C, with mean annual rainfall of 499 mm.

120 Contained within the Park is one of the six Exploratory platform sites contributing to  
121 FunDivEurope: Functional Significance of Biodiversity in European Forests (Baeten et al.,  
122 2013). Field data used in the current study were taken from plots surveyed as part of this  
123 programme. The landscape-level analysis focused on a belt overlapping this ~~area~~area and  
124 running 20 km north–south and 3 km east–west (Fig. 2).

## 2.2 Plot-based tree measurements and allometric biomass modelling

Field measurement of plots was undertaken in March 2012. Each plot was of dimension 30 x 30 m and was carefully geo-located, recording GPS corner coordinates and orientation using a Trimble GeoXT - Geoexplorer 2008. For each tree and shrub (diameter at breast height, DBH > 7.5 cm), the

Field measurement of plots was undertaken in March 2012. Each plot was of dimension 30 x 30 m and was carefully geo-located, recording GPS corner coordinates and orientation using a Trimble GeoXT - Geoexplorer 2008. Measurements were made of trees and shrubs of diameter at breast height (DBH) > 7.5 cm, given that smaller sizes contribute less to plot-level biomass (Stephenson et al., 2014). The following were measured and recorded: position within plot, species, height, height of lowest branch, DBH (at 1.3 m), and crown diameter (two orthogonal measurements). A vertex hypsometer was used for the crown dimensions.

The above ground biomass of individual trees was estimated according to published allometries, and summed to arrive at plot and hectare totals. The allometric equations of Ruiz-Peinado, del Rio, & Montero (2011) and Ruiz-Peinado, Montero, & del Rio (2012) were used for softwood species (*Juniperus* and *Pinus*) and hardwood species (*Quercus*), respectively (Appendix A). The equations were developed from tree samples across Spain including sites close to the Alto Tajo study area. The equations for *Juniperus thurifera* were applied to the other two junipers (*J. oxycedrus* and *J. phoenicia*) as well as box (*Buxus sempervirens*). In all cases, the equations compartmented the biomass into trunks and large, medium and fine branches/leaves, using DBH and tree height data.

## 2.3 Lidar surveys, calibration and above-ground biomass and carbon change analysis

The lidar surveys were undertaken by the NERC Airborne Research and Survey Facility (ARSF) and took place on 16 May 2006 (project WM06\_04; García et al., 2011, 2010) and 21 May 2011 (project CAM11\_03). A Dornier 228 aircraft was employed for both, but lidar instruments differed between years: Optech ALTM-3033 in 2006 and Leica ALS050 in 2011. Instrument and flight parameters are given in Table 1. Simultaneous GPS measurement was carried out on the ground allowing for differential correction during post-processing.

We assumed accurate georeferencing of the 2006 and 2011 datasets during post-processing, and did no further co-registration. We performed initial modelling of terrain and canopy heights from the 2006 and 2011 lidar datasets using 'Tiffs' 8.0: Toolbox for Lidar Data Filtering and Forest Studies, which employs a computationally efficient, grid-based morphological filtering method described by Chen et al. (2007). Outputs included filtered ground and object points, as well as digital terrain models (DTM) and canopy height models (CHM). The subsequent GIS and statistical analyses described below were undertaken in ArcInfo 10.0 (ESRI 2013) and R 2.13.1 (R Development Core Team, 2011), respectively.

Spatially overlaying the lidar dataset with land cover information derived from the 2006 CORINE map (EEA, 1995), indicated the local presence of two main forest types: coniferous and mixed (oak-juniper-pine) woodland. For the purposes of calibrating the lidar height models based on field-estimated biomass, only the latter forest type was adequately sampled

165 (13 plots), so subsequent analysis and modelling focused on these mixed woodland systems.  
166 We predicted biomass as a function of top-of-canopy heights, which has been found to be a  
167 good predictor (Asner et al., 2013). Digitised plot boundaries for the 13 FunDiv plots of  
168 square 30 x 30 m were used to extract mean top-of-canopy height values from the lidar CHM  
169 (TCH<sub>L</sub>). Reassuringly, these values were remarkably similar to the mean canopy height  
170 estimated from plot data (TCH<sub>P</sub>), calculated from height and crown area of each tree obtained  
171 by allometric formulae (see Kent *et al.* 2015); there was almost a 1:1 relationship between the  
172 two estimates of height:  $TCH_G = 1.79 + 0.999 \times TCH_L$  ( $R^2 = 0.88$ ). Field-estimated AGB was  
173 modelled on the basis of lidar mean height by linear regression of log transformed variables.  
174 Our selected model ( $\log(AGB) = 3.02 + 0.89 \cdot \log(TCH_L)$ ,  $R^2 = 0.53$ , RMSE = 0.28) was back-  
175 transformed and multiplied by a correction factor (CF) to account for the back-transformation  
176 of the regression error (Baskerville, 1972); the correction factor is given by  $CF = e^{MSE/2}$ ,  
177 where MSE is the mean square error of the regression model.

178 We used the regression model and lidar dataset to map biomass and biomass change. ~~We~~  
179 ~~aggregated canopy heights at 1 m resolution to mean values per 30 x 30 m grid cell, to reduce~~  
180 ~~mismatches with the field inventory plots (Réjou-Méchain et al., 2014).~~ ~~We aggregated~~  
181 ~~canopy heights at 1 m resolution to mean values per 30 x 30 m grid cell, to reduce mismatches~~  
182 ~~with the field inventory plots (Réjou-Méchain et al., 2015).~~ The aggregation was also  
183 effective in dealing with gappiness noted in the 2006 dataset due to uneven distribution of  
184 scan lines and lower point density (Table 1). Negative values caused by occasional  
185 inaccuracies evident in the DTM models, especially for 2006, were removed from the dataset  
186 to avoid anomalies. For each grid cell along the three north-south transects, we were able use  
187 the mean height-AGB regression relationship to generate estimates of AGB in 2006 and  
188 2011, and AGB change 2006-2011.

## 189 2.4 Validation

190 ~~We validated~~ ~~Due to the relatively low number of ground truth plots, it was especially~~  
191 ~~important to validate~~ the lidar-modelled AGB estimates, ~~and this was done~~ using two different  
192 datasets. Firstly, equivalent estimates of AGB and AGB change were developed using  
193 detailed tree measurements from the Spanish National Forest Inventory (SFI). The SFI covers  
194 the forested areas of the country on a 1-km<sup>2</sup> grid (Villanueva, 2004). A subset of 234 SFI  
195 plots surrounding the study area and of comparable topography and climate were selected,  
196 and the data extracted for the second and third surveys (2SFI, 1992-94 and 3SFI, 2003-2006;  
197 i.e. an 11-year interval for this region). For each, plot-level AGB was calculated by applying  
198 the allometric equations of Ruiz-Peinado et al (2011, 2012; Appendix A) to individual tree  
199 height and stem diameter measurements and summing these up to the plot level. Information  
200 on topoclimate (altitude, rainfall, temperature; Gonzalo 2008) and management/fire  
201 disturbance were also available per plot, although areas significantly burned after the first  
202 inventory were removed from the dataset.

203 Secondly, plot-level above-ground wood productivity values were calculated from tree-ring  
204 measurements from the same FunDiv plots used to calibrate the lidar data, according to a  
205 four-step procedure described in Jucker et al. (2014): measuring growth increments from



206 wood cores, converting diameter increments into biomass growth, modelling individual tree  
207 biomass growth, and scaling up to plot level. ~~In this approach, plot level estimates were based~~  
208 ~~on the growth of trees present in 2011 and did not account for the growth of trees that~~For the  
209 ~~coring, bark-to-pith increment cores were collected for a subset of trees in each plot (using a~~  
210 ~~5.15 mm diameter increment borer, Haglöf AB, Sweden). Following a size-stratified random~~  
211 ~~sampling approach, one core was extracted from each selected tree at a height of 1.3 m off the~~  
212 ~~ground; 12 trees per plot were cored in monocultures and 6 trees per species were cored in~~  
213 ~~mixtures (Jucker et al., 2014). In this approach, plot level estimates were based on the growth~~  
214 ~~of trees present in 2011 and did not account for the growth of trees that died between 1992~~  
215 ~~and 2011.~~  
216 ~~died between 1992 and 2011.~~

217  
218

## 219 **2.5 Biomass growth estimation and simulation modelling**

220 Plotting the 30 x 30 m pixel-level AGB estimates from 2006 versus 2011 revealed a small  
221 number of outliers of AGB change that may have resulted from anomalies in the DTM and  
222 top-of-canopy modelling (see discussion). We used robust regression to remove these outliers  
223 in order to obtain reliable estimates of mean growth and its uncertainty. This was performed  
224 with the *rlm* command in the *MASS* package of R, which uses iterative re-weighted least  
225 squares (M-estimation) (Venables and Ripley, 2002). Robust regression assigns lower weights  
226 to outliers than to points close to the regression line (in our case, using a bisquare weighting  
227 function), and then uses these weights to downplay the importance of these outliers in the  
228 linear regression. On inspection of the weights, we observed that all the obvious outliers had  
229 been assigned a weight of zero, so were easily filtered out.- Some 3.3% of the data were  
230 trimmed in this way. The residuals of the remaining dataset were close to normally  
231 distributed. Change in AGB was calculated for each plot in the trimmed dataset as  $(AGB_{2011}$   
232  $- AGB_{2006})/5$ , and the mean and standard deviation estimated. There was significant spatial  
233 auto-correlation of  $AGB_{2006}$  values (Moran's  $I = 0.138$ ,  $p < 0.001$ ) and also AGB change  
234 (Moran's  $I = 0.038$ ,  $p < 0.001$ ). However, following the conclusion of Hawkins et al. (2007)  
235 that regression estimates are not significantly affected by spatial autocorrelation, we  
236 considered it unnecessary to subsample the gridded dataset to avoid it.

237 The trimmed dataset was used to model AGB growth as a function of biomass, using  
238 Bayesian inference, and to create a woodland dynamics simulator. The growth model was:

$$239 \quad AGB_{2011} = a + b \times AGB_{2006} + \varepsilon \quad \text{where } \varepsilon \sim N(0, c + d \times AGB_{2006}) \quad (1)$$

240 where  $a$ ,  $b$ ,  $c$  and  $d$  are parameters calculated using STAN (STAN Development Team, 2014),  
241 a Bayesian inference package. We used uninformative prior and a burn-in of 5000 iterations  
242 (well in excess of that needed for convergence), then took 100 samples from the posterior  
243 distribution. We also fitted a model containing a quadratic biomass term, but the 95%  
244 confidence intervals of the quadratic term overlapped with zero, indicating no support for its  
245 inclusion.

246 Parameter values drawn from the posterior distribution were fed into a simple simulation  
247 model. We created a 5000 cell “landscape” with starting biomass sampled randomly from  
248 AGB<sub>2006</sub>. For each cell the annual biomass increments were estimated by drawing parameters  
249 randomly from the posterior distribution

$$250 \quad \Delta\text{AGB} = (a + (b - 1) \times \text{AGB} + \varepsilon)/5 \quad (2)$$

251 where  $\varepsilon$  was drawn at random from  $N(0, c + d \times \text{AGB})$ . The biomass of each cell was then  
252 altered by  $\Delta\text{AGB}$  and the iterative process continued for 100 years. Mean AGB values for the  
253 landscape each year were recorded and plotted with 95% confidence intervals.

254 We also included the effect of various fire scenarios on mean biomass change and carbon  
255 dynamics in a simplistic way. We assumed that the probability of a cell being destroyed by  
256 fire,  $p$ , did not depend on that cell’s AGB and did not vary among years. For each time step  
257 and pixel, we decided whether a fire event had occurred in a cell by drawing random numbers  
258 from the binomial distribution, with the AGB being reset to zero as a result of a fire event. An  
259 annual probability of fire occurrence for the region of Guadalajara, based on areas burned  
260 each year 1991–2010 (Ministerio de Agricultura, 2002, 2012) is  $p=0.002$ , whilst that from a  
261 model parameterized from topoclimatic data from southern Spain is  $p=0.004$  (Purves et al.,  
262 2007). A five-fold increase in area burned as a result of a high emission climate scenario is  
263 predicted for similar forest types in Portugal (see Carvalho et al. 2009). Thus, as well as the  
264 no-fire scenario, we tested the three fire probabilities of  $p=0.002$ , 0.004 and 0.01 to look at  
265 the sensitivity of carbon accumulation in the mixed woodlands to a realistic range of fire  
266 frequencies. Carbon sequestration potential (mean carbon storage in biomass over the  
267 simulation period, Mg/ha) was calculated using the IPCC default 0.47 carbon fraction  
268 (McGroddy, M.E., Daufresne and Hedin, 2004), and scaled up to a total value of carbon (and  
269 CO<sub>2</sub> equivalent, 3.67 x C, Mt) for all mixed woodland in the autonomous community of  
270 Castilla La Mancha (181,000 ha) under the no-fire and three fire scenarios. We acknowledge  
271 that the simulation model is basic, and since it is not spatially explicit it makes no  
272 consideration of landscape connectivity. However, the results provide insight into the likely  
273 effect of varying fire rates on carbon dynamics.

### 274 3. Results

275 Lidar estimated mean AGB of mixed woodlands was 41.8 Mg/ha in 2006 and 47.9 Mg/ha in  
276 2011. Mean biomass change in this five-year period was 1.22 Mg/ha/yr, with a considerable  
277 degree of variation around this estimate (SD = 1.92 Mg/ha) and a large number of pixels  
278 losing biomass (Fig. 3), presumably as a result of disturbance. There was very good  
279 agreement between above-ground biomass estimated from the lidar modelling and Spanish  
280 National Inventory plots for mixed oak-juniper-pine woodland (Table 2). The lidar-based  
281 estimate is also in reasonable agreement with that calculated from the 2006 dataset in an  
282 earlier analysis: 44.7 Mg/ha for holm oak woodland (García et al., 2010). AGB change as  
283 modelled by the lidar approach was also close to estimates derived from the SFI and the  
284 Fundiv tree ring data (Table 2). The standard deviation of the lidar-based AGB change  
285 estimate is relatively high, probably as a result of lidar sampling/processing errors that are

286 greater than measurement errors associated with plots and tree rings. From the lidar dataset,  
287 there was a statistically significant but minor effect on AGB change of altitude (range 908–  
288 1322 m;  $\Delta\text{AGB} = 21.17 - 0.01 \times \text{altitude}$ ,  $R^2 = 0.0180$ ,  $p < 0.001$ ) and aspect (calculated as  
289 folded aspect laspect–180;  $\Delta\text{AGB} = 3.31 - 0.03 \times \text{aspect}$ ,  $R^2 = 0.0057$ ,  $p < 0.001$ ).

290 Biomass change was modelled according to the relationship:

$$291 \text{AGB}_{2011} = 3.98 + 1.05 \times \text{AGB}_{2006} + \varepsilon \quad \text{where } \varepsilon \sim N(0, 4.32 + 1.10 \times \text{AGB}_{2006}) \quad (3)$$

292 Because  $b > 1$ , (i.e. With  $b = 1.05$ ) (i.e.  $> 1$ ), the woodlands are accumulating biomass over  
293 time, and although the variance term is large and so some cells are losing biomass (Fig.  
294 3). The disturbance-free simulation model showed a strong increase in accumulated AGB  
295 over the whole 100 year period (Fig. 4a). The mean AGB rose from 42.6 ( $\pm 5.6$ ) to 236.9 ( $\pm$   
296 18.5) Mg/ha, which equates to a mean carbon flux of 1.95 MgC/ha/yr. By modelling the  
297 occurrence of fire at probabilities of  $p = 0.002$ , 0.004 and 0.01, we showed its potential  
298 impact on biomass and therefore carbon accumulation (Fig. 4, Table 3). Mean (and standard  
299 deviation) values for AGB after 100 years were 200.6 ( $\pm 21.1$ ), 174.2 ( $\pm 22.7$ ), and 114.1 ( $\pm$   
300 21.5) Mg/ha for a fire probability of 0.002, 0.004 and 0.01 (or return rate of 500, 250 and 100  
301 years) respectively. The effects of increasing fire occurrence also have dramatic effects on the  
302 carbon sequestration potential of the mixed woodlands considered at a regional level (i.e.  
303 Castilla la Mancha, Table 3), with the most severe fire regime reducing that potential by  
304 almost a half.

Formatted: Font: Italic

305

#### 306 4. Discussion

307 Here we provide a demonstration of the potential of lidar remote sensing to deliver large-scale  
308 high-fidelity maps of above-ground biomass and carbon dynamics. Our lidar-based biomass  
309 growth model, estimating a mean annual growth of 1.22 MgC/ha/yr, is in excellent agreement  
310 with the estimate independently derived from the Spanish National Forest Inventory (1.19  
311 MgC/ha/yr). Even though there is a large standard deviation around our estimate, the  
312 enormous sample size (9136 pixels) means that standard errors become miniscule, so our  
313 landscape level projections are delivered with high precision and reliability (Coomes et al.,  
314 2002). The number of field sampling plots used to calibrate the lidar top-of-canopy model is  
315 statistically enough given the parameters calculated and, therefore, for the purposes of our  
316 study. The coefficient of determination of the resulting model ( $R^2 = 0.53$ ) can be compared  
317 with a value of 0.67 obtained by García et al. (2010) for the same region. The difference could  
318 be due to that fact that García et al. (2010) included more plots across a greater range of  
319 woodland types, heights and carbon densities.

320 In the Anthropocene era of rapid climate and environmental change, there is an urgent need  
321 for reliable large-scale monitoring of above-ground biomass and carbon stocks in forests and  
322 woodlands (Henry et al., 2015), and developing our understanding of how carbon stocks will  
323 change in the future. Forests serve the critical function of sequestering atmospheric carbon  
324 and reducing the potential rate of climate change. However, they also provide other highly

325 important services, including provision of timber, food and other non-timber products,  
326 regulation of water cycle and habitat for biodiversity (Gamfeldt et al., 2013; Ojea et al., 2012;  
327 WRI, 2005). The amount of biomass in forest is a metric relevant to all of these functions,  
328 with an especially close relationship with sequestered and stored carbon (Boisvenue and  
329 Running, 2006). In the context of climate change mitigation and emissions target agreements  
330 made at national level, robust methodologies are needed for the regular assessment of carbon  
331 stocks in forests (Gibbs et al., 2007).

332 Our work demonstrates one such robust approach that has delivered a credible model of  
333 landscape-level carbon stocks and fluxes based on a five-year interval repeat-survey lidar  
334 dataset. The methodology involved identifying and discarding a small number of outliers in  
335 the AGB estimates, and it is worth reflecting on their origin. One of the challenges of multi-  
336 temporal lidar analyses are when different instruments and specifications are used in the  
337 surveys. In our case, the 2006 lidar survey had a much lower point density than for 2011, and  
338 inspection of the resulting point cloud indicated a considerably uneven distribution of the scan  
339 lines. The accuracy of the resulting terrain and canopy models will therefore be lower,  
340 potentially giving rise to some of the anomalies in our results. We sought to quantify the  
341 source of this error by performing a comparison of top-of-canopy height (TCH) models from  
342 crossing flight-lines (data not given) for both years at the 30 m grid scale, for which the  
343 standard deviation for 2006 was more than double that for 2011. TCH is known to be quite  
344 robust across different instruments (Asner and Mascaro, 2014), being less susceptible to  
345 differences in laser canopy penetration than mean canopy height (MCH) (Næsset, 2009).  
346 ~~However, our plots are quite small and this means that~~We considered that the size of our plots  
347 ~~was sufficient for calibrating the system, though~~ in comparison with larger plots: (1) errors  
348 caused by spatial misalignment of plots and lidar data are greater (Asner et al., 2009); (2)  
349 integrating measurements provides a less representative average (Zolkos et al., 2013); and (3)  
350 disagreement in protocol between lidar and field observations is greater (influenced by the  
351 effects of bisecting tree crowns in lidar data versus calling a tree 'in' or 'out' of the plot in  
352 field data; Mascaro et al., 2011). With regard to the latter issue, the potential error is affected  
353 by the average crown size relative to plot dimensions, such that it will be less in our situation  
354 (as it also is for boreal forest, Næsset et al., 2011), than it would be for tropical forests.

355 At the extensive spatial scales required, remote sensing methodologies offer the only  
356 practicable approach to the challenge of forest monitoring, with lidar being the remote sensing  
357 instrument of choice given its potential to characterise the three dimensional structure of  
358 canopies and understories to a high degree of accuracy and resolution. Whilst spatial and  
359 temporal lidar coverage of the terrestrial and wooded surface of the planet is still limited,  
360 ~~this~~and the costs still high, this situation is improving continuously. A number of national  
361 surveys have been undertaken or commissioned, and building on the experience of the GLAS  
362 (Geoscience Laser Altimetry System) instrument on ICESAT (2003–2010), the GEDI Lidar  
363 space-borne facility is planned for deployment in 2019 (Dubayah et al., 2014). With these  
364 advancements, it is an important time to develop proof of principle of lidar monitoring of  
365 forest biomass and carbon stocks and fluxes. In this respect, a number of important multi-  
366 temporal lidar studies have emerged. Typical of these are an analysis of AGB dynamics, tree

367 growth and peat subsidence in peat swamp forests of Central Kalimantan, Indonesia 2007–  
368 2011 (Boehm et al., 2013; Englhart et al., 2013), biomass changes in conifer forests of  
369 northern Idaho 2003–2009 at the pixel, plot and landscape level and looking at the impacts of  
370 logging (Hudak et al., 2012), studies of canopy gap dynamics (Blackburn et al., 2014;  
371 Vepakomma et al., 2008, 2010, 2011), and treefall rates and spatial patterns in a savanna  
372 landscape 2008–2010 (Levick and Asner, 2013). A study employing four lidar surveys  
373 between 2000–2005 established an optimum interval (3 years) for measuring tree growth in  
374 red pine forests at an acceptable level of uncertainty (Hopkinson et al., 2008).

375 Our study makes an important additional contribution to this literature. It demonstrates how a  
376 relatively low-intensive field-sampling campaign woodland system with a small number of  
377 field plots can effectively calibrate a lidar dataset to scale up credible estimates of AGB and  
378 AGC at the landscape level. It is also novel in studying these dynamics within a  
379 Mediterranean environment. Much focus of lidar-based biomass modelling has been on  
380 tropical forest systems, given their importance to the global carbon cycle. Mediterranean  
381 woodlands hold a much lower carbon density, yet are valuable carbon stores given their  
382 extensive nature not just in the Mediterranean Basin but also other similar climate regions in  
383 the world. Furthermore, the potential effects of climate change in Mediterranean woodlands  
384 are suggested to be particularly strong (Benito-Garzón et al., 2013; Ruiz-Benito et al., 2014b).  
385 In the absence of fire in one such region, our simulation suggests a significant AGB increase  
386 from 42.6 to 236.9 Mg/ha over a 100 year period (equivalent to 1.94 MgC/ha/yr). Pan et al.  
387 (2011) estimates an annual increase of 1.68 MgC/ha/yr in European temperate forests in  
388 2000–2007, whilst the annual carbon sink in Mediterranean pine plantations range between  
389 1.06–2.99 MgC/ha/yr depending on species and silvicultural treatment (Bravo et al., 2008).  
390 Estimates provided by Ruiz-Benito et al. (2014) range from 0.55 (sclerophyllous vegetation)  
391 to 0.73 (natural pine forest) and 1.45 (pine plantation). Our own estimate of carbon  
392 sequestration potential equates to a regional carbon sequestration potential of over 10 M kg  
393 (19 kt CO<sub>2</sub> equivalent) for mixed woodlands in Castilla la Mancha. Such a figure can be set in  
394 the context of national level commitments to the reduction of greenhouse gas emissions of  
395 10% against the Kyoto base year value of 289.8 Mt CO<sub>2</sub> equivalent (EEA, 2014). Under  
396 Spain's 'Socioeconomic Plan of Forest Activation', land use, land use change and forestry  
397 (LULUCF) is projected to absorb 20–30 Mt CO<sub>2</sub> equivalent per year.

398 The contribution of Mediterranean forests to the greenhouse gas balance sheet is vulnerable to  
399 the effects of climate change, for which the Mediterranean is a hotspot region (Giorgi and  
400 Lionello, 2008; Lindner et al., 2010). One of the mediating drivers is forest fire risk. We  
401 found that an increase in fire probability from 0.002 to 0.01 (return rate increase from 500 to  
402 100 years) dramatically altered the carbon sequestration potential of the landscape, with  
403 carbon stocks much reduced after 100 years with the highest fire probability scenario. It is  
404 worth noting in this respect that our modelled range of fire probabilities are conservative  
405 compared to estimates used in other simulations for similar regions (e.g. 0.01–0.2 for  
406 Catalonia, Lloret et al., 2003). However, it is also necessary to note that our simplistic  
407 modelling of fire, using a set probability of a burn irrespective of factors such as landscape  
408 position and temporal variability, mean that our results can only be treated as indicative of the

409 scale of effect of different scenarios on the landscape carbon dynamics. For example, our  
410 modelling does not account for the way in which small changes in temperature and rainfall  
411 regimes could lead to tipping points of much higher risk and frequency, if not severity, of  
412 burns (Moritz et al., 2012), and dramatically different carbon dynamics outcomes.

413 Our modelling is neither able to account for ecophysiological factors. Tree physiology is  
414 responsive to changing temperature and soil water availability, influencing rates of  
415 regeneration, growth and mortality (Choat and Way, 2013; Choat et al., 2012; Frank et al.,  
416 2015; Williams et al., 2012). One study of low productivity forests (including Alto Tajo as a  
417 continental Mediterranean study area) showed how leaf respiration rates, and their ability to  
418 acclimate to seasonal changes in the environment, have a profound effect on whether trees can  
419 maintain productivity – and continue to act as carbon sinks – in dryland areas (Zaragoza-  
420 Castells et al., 2008).

421 Nevertheless, our modelling approach shows considerable promise for understanding the  
422 effects of different drivers on vegetation dynamics and making informative future predictions  
423 (Chambers et al., 2013; Coomes and Allen, 2007; Espírito-Santo et al., 2014). We compared  
424 no-fire with three different fire scenarios, but it would be equally possible to develop our  
425 approach further to consider other environmental and ecological drivers of the AGB and AGC  
426 dynamics, including tree diversity (Jucker et al., 2014; Ruiz-Benito et al., 2014a) and  
427 competition effects (Ruiz-Benito et al., 2014a, 2014b; Vayreda et al., 2012). With regard to  
428 understanding the landscape-level carbon dynamics of Spanish forests, in further work we  
429 propose coverage of a full range of different forest types and the development of more  
430 sophisticated climate change scenarios using models based on meteorological data,  
431 environmental parameters and different IPCC projections. More widely, the further  
432 development and testing of these methods is critical for exploring the prospects for, and  
433 contribution of, forests in the global carbon cycle under future environmental change.

#### 434 **Author contributions**

435 The project was conceived by DAC and WDS. Lidar analysis and first manuscript drafting  
436 was undertaken by WDS. DAC designed the statistical approach, and PRB provided the  
437 independent validation data and analysis based on the Spanish National Forest Inventory. FV  
438 oversaw field data collection, and with all authors contributed to the finalisation of the  
439 manuscript.

#### 440 **Acknowledgements**

441 Field data were collected by T. Jucker and partners from University Stefan cel Mare of  
442 Suceava (Romania) and National Museum of Natural Sciences, Madrid (Spain). Biomass  
443 estimates were calculated by T. Jucker. The authors would like to acknowledge the personnel  
444 of the Airborne Research and Survey Facility (NERC). We thank the MAGRAMA for  
445 granting access to the Spanish Forest Inventory. WS was funded by FunDivEurope and the  
446 Isaac Newton Trust. PRB was supported by The International Post doc Fellowship  
447 Programme in Plant Sciences (PLANT FELLOWS).

448

449 **6. References**

- 450 Allen, C. D., Macalady, A. K., Chenchouni, H., Bachelet, D., McDowell, N., Vennetier, M.,  
451 Kitzberger, T., Rigling, A., Breshears, D. D., Hogg, E. H. (Ted), Gonzalez, P., Fensham, R.,  
452 Zhang, Z., Castro, J., Demidova, N., Lim, J.-H., Allard, G., Running, S. W., Semerci, A. and  
453 Cobb, N.: A global overview of drought and heat-induced tree mortality reveals emerging  
454 climate change risks for forests, *For. Ecol. Manage.*, 259(4), 660–684,  
455 doi:10.1016/j.foreco.2009.09.001, 2010.
- 456 Asner, G. P. and Mascaro, J.: Mapping tropical forest carbon: Calibrating plot estimates to a  
457 simple LiDAR metric, *Remote Sens. Environ.*, 140, 614–624, doi:10.1016/j.rse.2013.09.023,  
458 2014.
- 459 Asner, G. P., Flint Hughes, R., Varga, T. A. , Knapp, D. E. and Kennedy-Bowdoin, T.:  
460 Environmental and Biotic Controls over Aboveground Biomass Throughout a Tropical Rain  
461 Forest, *Ecosystems*, 12, 261–278, doi:10.1007/s10021-008-9221-5, 2009.
- 462 Asner, G. P., Mascaro, J., Anderson, C., Knapp, D. E., Martin, R. E., Kennedy-Bowdoin, T.,  
463 van Breugel, M., Davies, S., Hall, J. S., Muller-Landau, H. C., Potvin, C., Sousa, W., Wright,  
464 J. and Bermingham, E.: High-fidelity national carbon mapping for resource management and  
465 REDD+, *Carbon Balance Manag.*, 8(1), 7, doi:10.1186/1750-0680-8-7, 2013.
- 466 Baeten, L., Verheyen, K., Wirth, C., Bruelheide, H., Bussotti, F., Finér, L., Jaroszewicz, B.,  
467 Selvi, F., Valladares, F., Allan, E., Ampoorter, E., Auge, H., Avăcăriei, D., Barbaro, L.,  
468 Bărnoaiea, I., Bastias, C. C., Bauhus, J., Beinhoff, C., Benavides, R., Benneter, A., Berger, S.,  
469 Berthold, F., Boberg, J., Bonal, D., Brüggemann, W., Carnol, M., Castagneyrol, B.,  
470 Charbonnier, Y., Chećko, E., Coomes, D., Coppi, A., Dalmaris, E., Dănilă, G., Dawud, S. M.,  
471 de Vries, W., De Wandeler, H., Deconchat, M., Domisch, T., Duduman, G., Fischer, M.,  
472 Fotelli, M., Gessler, A., Gimeno, T. E., Granier, A., Grossiord, C., Guyot, V., Hantsch, L.,  
473 Hättenschwiler, S., Hector, A., Hermy, M., Holland, V., Jactel, H., Joly, F.-X., Jucker, T.,  
474 Kolb, S., Koricheva, J., Lexer, M. J., Liebergesell, M., Milligan, H., Müller, S., Muys, B.,  
475 Nguyen, D., Nichiforel, L., Pollastrini, M., Proulx, R., Rabasa, S., Radoglou, K., Ratcliffe, S.,  
476 Raulund-Rasmussen, K., Seiferling, I., Stenlid, J., Vesterdal, L., von Wilpert, K., Zavala, M.  
477 a., Zielinski, D. and Scherer-Lorenzen, M.: A novel comparative research platform designed  
478 to determine the functional significance of tree species diversity in European forests, *Perspect.*  
479 *Plant Ecol. Evol. Syst.*, 15(5), 281–291, doi:10.1016/j.ppees.2013.07.002, 2013.
- 480 Baskerville, G. L.: Regression in the Estimation of Plant Biomass, *Can. J. For.*, 2, 49–53,  
481 doi:Export Date 18 February 2014, 1972.
- 482 Benito-Garzón, M., Ruiz-Benito, P. and Zavala, M. a.: Interspecific differences in tree growth  
483 and mortality responses to environmental drivers determine potential species distributional  
484 limits in Iberian forests, *Glob. Ecol. Biogeogr.*, 22(10), 1141–1151, doi:10.1111/geb.12075,  
485 2013.
- 486 Blackburn, G. A., Abd Latif, Z. and Boyd, D. S.: Forest disturbance and regeneration: a  
487 mosaic of discrete gap dynamics and open matrix regimes?, edited by T. Nakashizuka, *J. Veg.*  
488 *Sci.*, n/a–n/a, doi:10.1111/jvs.12201, 2014.

489 Boehm, H.-D. V., Liesenberg, V. and Limin, S. H.: Multi-Temporal Airborne LiDAR-Survey  
490 and Field Measurements of Tropical Peat Swamp Forest to Monitor Changes, *IEEE J. Sel.*  
491 *Top. Appl. Earth Obs. Remote Sens.*, 6(3), 1524–1530, doi:10.1109/JSTARS.2013.2258895,  
492 2013.

493 Boisvenue, C. and Running, S. W.: Impacts of climate change on natural forest productivity -  
494 Evidence since the middle of the 20th century, *Glob. Chang. Biol.*, 12, 862–882,  
495 doi:10.1111/j.1365-2486.2006.01134.x, 2006.

496 Bravo, F., Bravo-Oviedo, a. and Diaz-Balteiro, L.: Carbon sequestration in Spanish  
497 Mediterranean forests under two management alternatives: a modeling approach, *Eur. J. For.*  
498 *Res.*, 127(3), 225–234, doi:10.1007/s10342-007-0198-y, 2008.

499 Carvalho, A., Flannigan, M. D., Logan, K. a., Gowman, L. M., Miranda, A. I. and Borrego,  
500 C.: The impact of spatial resolution on area burned and fire occurrence projections in Portugal  
501 under climate change, *Clim. Change*, 98, 177–197, doi:10.1007/s10584-009-9667-2, 2009.

502 Chambers, J. Q., Negron-Juarez, R. I., Marra, D. M., Di Vittorio, A., Tews, J., Roberts, D.,  
503 Ribeiro, G. H. P. M., Trumbore, S. E. and Higuchi, N.: The steady-state mosaic of disturbance  
504 and succession across an old-growth Central Amazon forest landscape., *Proc. Natl. Acad. Sci.*  
505 *U. S. A.*, 110(10), 3949–54, doi:10.1073/pnas.1202894110, 2013.

506 Chen, Q., Gong, P., Baldocchi, D. and Xie, G.: Filtering Airborne Laser Scanning Data with  
507 Morphological Methods, *Photogramm. Eng. Remote Sens.*, 73(2), 175–185, 2007.

508 Choat, B. and Way, D.: Predicting thresholds of drought-induced mortality in woody plant  
509 species, *Tree Physiol.*, 33(2009), 669–671, doi:10.1093/treephys/tpt046, 2013.

510 Choat, B., Jansen, S., Brodribb, T. J., Cochard, H., Delzon, S., Bhaskar, R., Bucci, S. J., Feild,  
511 T. S., Gleason, S. M., Hacke, U. G., Jacobsen, A. L., Lens, F., Maherali, H., Martínez-Vilalta,  
512 J., Mayr, S., Mencuccini, M., Mitchell, P. J., Nardini, A., Pittermann, J., Pratt, R. B., Sperry,  
513 J. S., Westoby, M., Wright, I. J. and Zanne, A. E.: Global convergence in the vulnerability of  
514 forests to drought., *Nature*, 491(7426), 752–5, doi:10.1038/nature11688, 2012.

515 Coomes, D. a. and Allen, R. B.: Effects of size, competition and altitude on tree growth, *J.*  
516 *Ecol.*, 95(5), 1084–1097, doi:10.1111/j.1365-2745.2007.01280.x, 2007.

517 Coomes, D. A., Allen, R. B., Scott, N. A., Goulding, C. and Beets, P.: Designing systems to  
518 monitor carbon stocks in forests and shrublands, *For. Ecol. Manage.*, 164(1-3), 89–108,  
519 doi:10.1016/S0378-1127(01)00592-8, 2002.

520 Drake, J. B., Knox, R. G., Dubayah, R. O., Clark, D. B., Condit, R., Blair, J. B. and Hofton,  
521 M.: Above-ground biomass estimation in closed canopy Neotropical forests using lidar  
522 remote sensing: factors, *Glob. Ecol. Biogeogr.*, 12, 147– 159, 2003.

523 Dubayah, R., Goetz, S. J., Blair, J. B., Fatoyinbo, T. E., Hansen, M., Healey, S. P., Hofton, M.  
524 A., Hurr, G. C., Kellner, J., Luthcke, S. B. and Swatantran, A.: The Global Ecosystem  
525 Dynamics Investigation, in *Proceedings of the American Geophysical Union.*, 2014.

526 EEA: CORINE Land Cover Project, Copenhagen., 1995.



527 EEA: Annual European Union greenhouse gas inventory 1990–2012 and inventory report  
528 2014 – EEA Technical Report No, 9/2014, European Environment Agency., 2014.

529 Englhart, S., Jubanski, J. and Siegert, F.: Quantifying Dynamics in Tropical Peat Swamp  
530 Forest Biomass with Multi-Temporal LiDAR Datasets, *Remote Sens.*, 5(5), 2368–2388,  
531 doi:10.3390/rs5052368, 2013.

532 Espírito-Santo, F. D. B., Gloor, M., Keller, M., Malhi, Y., Saatchi, S., Nelson, B., Junior, R.  
533 C. O., Pereira, C., Lloyd, J., Frohking, S., Palace, M., Shimabukuro, Y. E., Duarte, V.,  
534 Mendoza, A. M., López-González, G., Baker, T. R., Feldpausch, T. R., Brienen, R. J. W.,  
535 Asner, G. P., Boyd, D. S. and Phillips, O. L.: Size and frequency of natural forest disturbances  
536 and the Amazon forest carbon balance., *Nat. Commun.*, 5, 3434, doi:10.1038/ncomms4434,  
537 2014.

538 Frank, D., Reichstein, M., Bahn, M., Frank, D., Mahecha, M. D., Smith, P., Thonicke, K., van  
539 der Velde, M., Vicca, S., Babst, F., Beer, C., Buchmann, N., Canadell, J. G., Ciais, P.,  
540 Cramer, W., Ibrom, A., Miglietta, F., Poulter, B., Rammig, A., Seneviratne, S. I., Walz, A.,  
541 Wattenbach, M., Zavala, M. a and Zscheischler, J.: Effects of climate extremes on the  
542 terrestrial carbon cycle: concepts, processes and potential future impacts, *Glob. Chang. Biol.*,  
543 (January), n/a–n/a, doi:10.1111/gcb.12916, 2015.

544 Gamfeldt, L., Snäll, T., Bagchi, R., Jonsson, M., Gustafsson, L., Kjellander, P., Ruiz-Jaen, M.  
545 C., Fröberg, M., Stendahl, J., Philipson, C. D., Mikusiński, G., Andersson, E., Westerlund, B.,  
546 Andrén, H., Moberg, F., Moen, J. and Bengtsson, J.: Higher levels of multiple ecosystem  
547 services are found in forests with more tree species., *Nat. Commun.*, 4, 1340,  
548 doi:10.1038/ncomms2328, 2013.

549 García, M., Riaño, D., Chuvieco, E. and Danson, F. M.: Estimating biomass carbon stocks for  
550 a Mediterranean forest in central Spain using LiDAR height and intensity data, Elsevier Inc.,  
551 2010.

552 García, M., Riaño, D., Chuvieco, E., Salas, J. and Danson, F. M.: Multispectral and LiDAR  
553 data fusion for fuel type mapping using Support Vector Machine and decision rules, *Remote  
554 Sens. Environ.*, 115(6), 1369–1379, doi:10.1016/j.rse.2011.01.017, 2011.

555 Gibbs, H. K., Brown, S., Niles, J. O. and Foley, J. a: Monitoring and estimating tropical forest  
556 carbon stocks: making REDD a reality, *Environ. Res. Lett.*, 2, 045023, doi:10.1088/1748-  
557 9326/2/4/045023, 2007.

558 Giorgi, F. and Lionello, P.: Climate change projections for the Mediterranean region, *Glob.  
559 Planet. Change*, 63, 90–104, doi:10.1016/j.gloplacha.2007.09.005, 2008.

560 Gonzalo, J.: Diagnóstico fitoclimático de la España peninsular. Actualización y análisis  
561 geostadístico aplicado. Silvopascicultura, Madrid., 2008.

562 Hawkins, B. a., Diniz-Filho, J. A. F., Mauricio Bini, L., De Marco, P. and Blackburn, T. M.:  
563 Red herrings revisited: Spatial autocorrelation and parameter estimation in geographical  
564 ecology, *Ecography (Cop.)*, 30(May), 375–384, doi:10.1111/j.2007.0906-7590.05117.x,  
565 2007.

Formatted: Spanish (Spain)

566 Henry, M., Réjou-Méchain, M., Jara, M. C., Wayson, C., Piotto, D., Westfall, J., Fuentes, J.  
567 M. M., Guier, F. A., Lombis, H. C., López, E. C., Lara, R. C., Rojas, K. C., Del Águila  
568 Pasquel, J., Montoya, Á. D., Vega, J. F., Galo, A. J., López, O. R., Marklund, L. G., Milla, F.,  
569 de Jesús Návar Cahidez, J., Malavassi, E. O., Pérez, J., Zea, C. R., García, L. R., Pons, R. R.,  
570 Sanquetta, C., Scott, C., Zapata-Cuartas, M. and Saint-André, L.: An overview of existing and  
571 promising technologies for national forest monitoring, *Ann. For. Sci.*, doi:10.1007/s13595-  
572 015-0463-z, 2015.

573 Hopkinson, C., Chasmer, L. and Hall, R. J.: The uncertainty in conifer plantation growth  
574 prediction from multi-temporal lidar datasets, *Remote Sens. Environ.*, 112(3), 1168–1180,  
575 doi:10.1016/j.rse.2007.07.020, 2008.

576 Hudak, A. T., Strand, E. K., Vierling, L. a., Byrne, J. C., Eitel, J. U. H., Martinuzzi, S. and  
577 Falkowski, M. J.: Quantifying aboveground forest carbon pools and fluxes from repeat  
578 LiDAR surveys, *Remote Sens. Environ.*, 123, 25–40, doi:10.1016/j.rse.2012.02.023, 2012.

579 Jucker, T., Bouriaud, O., Avacaritei, D. and Coomes, D. a.: Stabilizing effects of diversity on  
580 aboveground wood production in forest ecosystems: linking patterns and processes, *Ecol.*  
581 *Lett.*, 17, 1560–1569, doi:10.1111/ele.12382, 2014.

582 Kellner, J. R. and Asner, G. P.: Winners and losers in the competition for space in tropical  
583 forest canopies., *Ecol. Lett.*, 17(5), 556–62, doi:10.1111/ele.12256, 2014.

584 Lefsky, M. A., Cohen, W. B., Harding, D. J., Parker, G. G., Acker, S. A. and Gower, S. T.:  
585 Lidar remote sensing of above-ground biomass in three biomes, *Glob. Ecol. Biogeogr.*, 11,  
586 393–399, 2002.

587 Levick, S. R. and Asner, G. P.: The rate and spatial pattern of treefall in a savanna landscape,  
588 *Biol. Conserv.*, 157, 121–127, doi:10.1016/j.biocon.2012.07.009, 2013.

589 Lindner, M., Maroschek, M., Netherer, S., Kremer, A., Barbati, A., Garcia-Gonzalo, J., Seidl,  
590 R., Delzon, S., Corona, P. and Kolström, M.: Climate change impacts, adaptive capacity, and  
591 vulnerability of European forest ecosystems, *For. Ecol. Manage.*, 259(4), 698–709,  
592 doi:10.1016/j.foreco.2009.09.023, 2010.

593 Lloret, F., Pausas, J. G. and Vila, M.: Responses of Mediterranean Plant Species to different  
594 fire frequencies in Garraf Natural Park (Catalonia, Spain): field observations and modelling  
595 predictions., *Plant Ecol.*, 167, 223–235, 2003.

596 Mascaro, J., Asner, G. P., Muller-Landau, H. C., Van Breugel, M., Hall, J. and Dahlin, K.:  
597 Controls over aboveground forest carbon density on Barro Colorado Island, Panama,  
598 *Biogeosciences*, 8, 1615–1629, doi:10.5194/bg-8-1615-2011, 2011.

599 McGroddy, M.E., Daufresne, T. and Hedin, L. O.: Scaling of C:N:P stoichiometry in forests  
600 worldwide: implications of terrestrial redfield-type ratios, *Ecology*, 85(9), 2390–2401, 2004.

601 Ministerio de Agricultura, A. y M. A.: Los Incendios Forestales en España Decenio 1991-  
602 2000, 2002.

Formatted: Spanish (Spain)

603 Ministerio de Agricultura, A. y M. A.: Los Incendios Forestales en España Decenio 2001-  
604 2010, 2012.

605 Moritz, M. a., Parisien, M.-A., Batllori, E., Krawchuk, M. a., Van Dorn, J., Ganz, D. J. and  
606 Hayhoe, K.: Climate change and disruptions to global fire activity, *Ecosphere*, 3(June), art49,  
607 doi:10.1890/ES11-00345.1, 2012.

608 Nabuurs, G. J., Schelhaas, M. J., Mohren, G. M. J. and Field, C. B.: Temporal evolution of the  
609 European forest sector carbon sink from 1959 to 1999, *Glob. Chang. Biol.*, 9, 152–160, 2003.

610 Nabuurs, G. J., Hengeveld, G. M., van der Werf, D. C. and Heidema, a. H.: European forest  
611 carbon balance assessed with inventory based methods-An introduction to a special section,  
612 *For. Ecol. Manage.*, 260(3), 239–240, doi:10.1016/j.foreco.2009.11.024, 2010.

613 Nabuurs, G.-J., Lindner, M., Verkerk, P. J., Gunia, K., Deda, P., Michalak, R. and Grassi, G.:  
614 First signs of carbon sink saturation in European forest biomass, *Nat. Clim. Chang.*, 3(9),  
615 792–796, doi:10.1038/nclimate1853, 2013.

616 Næsset, E.: Effects of different sensors, flying altitudes, and pulse repetition frequencies on  
617 forest canopy metrics and biophysical stand properties derived from small-footprint airborne  
618 laser data, *Remote Sens. Environ.*, 113(1), 148–159, doi:10.1016/j.rse.2008.09.001, 2009.

619 Næsset, E., Gobakken, T., Solberg, S., Gregoire, T. G., Nelson, R., Ståhl, G. and Weydahl,  
620 D.: Model-assisted regional forest biomass estimation using LiDAR and InSAR as auxiliary  
621 data: A case study from a boreal forest area, *Remote Sens. Environ.*, 115(12), 3599–3614,  
622 doi:10.1016/j.rse.2011.08.021, 2011.

623 Ojea, E., Ruiz-Benito, P., Markandya, A. and Zavala, M. a.: Wood provisioning in  
624 Mediterranean forests: A bottom-up spatial valuation approach, *For. Policy Econ.*, 20, 78–88,  
625 doi:10.1016/j.forpol.2012.03.003, 2012.

626 Pan, Y., Birdsey, R. a, Fang, J., Houghton, R., Kauppi, P. E., Kurz, W. a, Phillips, O. L.,  
627 Shvidenko, A., Lewis, S. L., Canadell, J. G., Ciais, P., Jackson, R. B., Pacala, S. W.,  
628 McGuire, a D., Piao, S., Rautiainen, A., Sitch, S. and Hayes, D.: A large and persistent carbon  
629 sink in the world’s forests., *Science*, 333, 988–993, doi:10.1126/science.1201609, 2011.

630 Pausas, J. G., Llovet, J., Anselm, R. and Vallejo, R.: Are wildfires a disaster in the  
631 Mediterranean basin ? – A review Vegetation changes Shrublands dominated by resprouting  
632 species, *Int. J. Wildl. Fire*, 17, 713–723, 2008.

633 Purves, D. W., Zavala, M. a., Ogle, K., Prieto, F. and Rey Benayas, J. M.: Environmental  
634 heterogeneity, bird-mediated directed dispersal, and oak woodland dynamics in  
635 Mediterranean Spain, *Ecol. Monogr.*, 77(1), 77–97, doi:10.1890/05-1923, 2007.

636 Réjou-Méchain, M., Muller-Landau, H. C., Detto, M., Thomas, S. C., Le Toan, T., Saatchi, S.,  
637 Barreto-Silva, J. S., Bourg, N. a., Bunyavejehewin, S., Butt, N., Broekelman, W. Y., Cao,  
638 M., Cárdenas, D., Chiang, J. M., Chuyong, G. B., Clay, K., Condit, R., Dattaraja, H. S.,  
639 Davies, S. J., Duque, a., Esufali, S., Ewango, C., Fernando, R. H. S., Fletcher, C. D.,  
640 Gunatilleke, I. a. U. N., Hao, Z., Harms, K. E., Hart, T. B., Hérault, B., Howe, R. W.,  
641 Hubbell, S. P., Johnson, D. J., Kenfaek, D., Larson, a. J., Lin, L., Lin, Y., Lutz, J. a., Makana,

642 [J. R., Malhi, Y., Marthews, T. R., McEwan, R. W., McMahon, S. M., McShea, W. J.,](#)  
643 [Muscarella, R., Nathalang, a., Noor, N. S. M., Nyteh, C. J., Oliveira, a. a., Phillips, R. P.,](#)  
644 [Pongpattananurak, N., Punchi-Manager, R., Salim, R., Schurman, J., Sukumar, R., Suresh, H.](#)  
645 [S., Suwanvecho, U., Thomas, D. W., Thompson, J., Uriarte, M., Valencia, R., Vicentini, a.,](#)  
646 [Wolf, a. T., Yap, S., Yuan, Z., Zartman, C. E., Zimmerman, J. K. and Chave, J.: Local spatial](#)  
647 [structure of forest biomass and its consequences for remote sensing of carbon stocks,](#)  
648 [Biogeosciences, 11\(23\), 6827–6840, doi:10.5194/bg-11-6827-2014, 2014](#)[Tymen, B., Blanc,](#)  
649 [L., Fauset, S., Feldpausch, T. R., Monteagudo, A., Phillips, O. L., Richard, H. and Chave, J.:](#)  
650 [Using repeated small-footprint LiDAR acquisitions to infer spatial and temporal variations of](#)  
651 [a high-biomass Neotropical forest, Remote Sens. Environ., 169, 93–101,](#)  
652 [doi:10.1016/j.rse.2015.08.001, 2015.](#)

653 Ruiz-Benito, P., Gómez-Aparicio, L., Paquette, A., Messier, C., Kattge, J. and Zavala, M. a.:  
654 Diversity increases carbon storage and tree productivity in Spanish forests, *Glob. Ecol.*  
655 *Biogeogr.*, 23(3), 311–322, doi:10.1111/geb.12126, 2014a.

656 Ruiz-Benito, P., Madrigal-González, J., Ratcliffe, S., Coomes, D. a, Kändler, G., Lehtonen, a.,  
657 Wirth, C. and Zavala, M. a.: Stand Structure and Recent Climate Change Constrain Stand  
658 Basal Area Change in European Forests: A Comparison Across Boreal, Temperate, and  
659 Mediterranean Biomes, *Ecosystems*, 1439–1454, doi:10.1007/s10021-014-9806-0, 2014b.

660 Ruiz-Peinado, R., del Rio, M. and Montero, G.: New models for estimating the carbon sink  
661 capacity of Spanish softwood species, *For. Syst.*, 20(1), 176–188, 2011.

662 Ruiz-Peinado, R., Montero, G. and del Rio, M.: Biomass models to estimate carbon stocks for  
663 hardwood tree species, *For. Syst.*, 21(1), 42–52, 2012.

664 Smith, M. J., Vanderwel, M. C., Lyutsarev, V., Emmott, S. and Purves, D. W.: The climate  
665 dependence of the terrestrial carbon cycle; including parameter and structural uncertainties,  
666 *Biogeosciences Discuss.*, 9, 13439–13496, doi:10.5194/bgd-9-13439-2012, 2012.

667 [Stephenson, N. L., Das, a. J., Condit, R., Russo, S. E., Baker, P. J., Beckman, N. G., Coomes,](#)  
668 [D. a., Lines, E. R., Morris, W. K., Rüger, N., Álvarez, E., Blundo, C., Bunyavejchewin, S.,](#)  
669 [Chuyong, G., Davies, S. J., Duque, Á., Ewango, C. N., Flores, O., Franklin, J. F., Grau, H. R.,](#)  
670 [Hao, Z., Harmon, M. E., Hubbell, S. P., Kenfack, D., Lin, Y., Makana, J.-R., Malizia, a.,](#)  
671 [Malizia, L. R., Pabst, R. J., Pongpattananurak, N., Su, S.-H., Sun, I.-F., Tan, S., Thomas, D.,](#)  
672 [van Mantgem, P. J., Wang, X., Wiser, S. K. and Zavala, M. a.: Rate of tree carbon](#)  
673 [accumulation increases continuously with tree size, Nature, 507\(7490\), 90–93,](#)  
674 [doi:10.1038/nature12914, 2014.](#)

675 Valladares, F., Benavides, R., Rabasa, S. G., Pausas, J. G., Paula, S., Simonson, W. D. and  
676 Diaz, M.: Global change and Mediterranean forests: current impacts and potential responses,  
677 in *Forests and Global Change*, pp. 47–76, Cambridge University Press, Cambridge, UK.,  
678 2014.

679 Vanderwel, M. C., Coomes, D. a. and Purves, D. W.: Quantifying variation in forest  
680 disturbance, and its effects on aboveground biomass dynamics, across the eastern United  
681 States, *Glob. Chang. Biol.*, 19, 1504–1517, doi:10.1111/gcb.12152, 2013.

682 Vayreda, J., Martínez-Vilalta, J., Gracia, M. and Retana, J.: Recent climate changes interact  
683 with stand structure and management to determine changes in tree carbon stocks in Spanish  
684 forests, *Glob. Chang. Biol.*, 18, 1028–1041, doi:10.1111/j.1365-2486.2011.02606.x, 2012.

685 Venables, W. N. and Ripley, B. D.: *Modern Applied Statistics with S*, Fourth edi., Springer,  
686 New York., 2002.

687 Vepakomma, U., St-Onge, B. and Kneeshaw, D.: Spatially explicit characterization of boreal  
688 forest gap dynamics using multi-temporal lidar data, *Remote Sens. Environ.*, 112(5), 2326–  
689 2340, doi:10.1016/j.rse.2007.10.001, 2008.

690 Vepakomma, U., Kneeshaw, D. and St-Onge, B.: Interactions of multiple disturbances in  
691 shaping boreal forest dynamics: a spatially explicit analysis using multi-temporal lidar data  
692 and high-resolution imagery, *J. Ecol.*, 98(3), 526–539, doi:10.1111/j.1365-  
693 2745.2010.01643.x, 2010.

694 Vepakomma, U., St-Onge, B. and Kneeshaw, D.: Response of a boreal forest to canopy  
695 opening: assessing vertical and lateral tree growth with multi-temporal lidar data., *Ecol.*  
696 *Appl.*, 21(1), 99–121 [online] Available from:  
697 <http://www.ncbi.nlm.nih.gov/pubmed/21516891>, 2011.

698 Villanueva, J. A.: *Tercer Inventario Forestal Nacional (1997–2007)*., Madrid., 2004.

699 Williams, A. P., Allen, C. D., Macalady, A. K., Griffin, D., Woodhouse, C. a., Meko, D. M.,  
700 Swetnam, T. W., Rauscher, S. a., Seager, R., Grissino-Mayer, H. D., Dean, J. S., Cook, E. R.,  
701 Gangodagamage, C., Cai, M. and McDowell, N. G.: Temperature as a potent driver of  
702 regional forest drought stress and tree mortality, *Nat. Clim. Chang.*, 3(3), 292–297,  
703 doi:10.1038/nclimate1693, 2012.

704 WRI: *Millennium Ecosystem Assessment. Ecosystem and human well-being: biodiversity*  
705 *synthesis*, , 86, 2005.

706 Zaragoza-Castells, J., Sánchez-Gómez, D., Hartley, I. P., Matesanz, S., Valladares, F., Lloyd,  
707 J. and Atkin, O. K.: Climate-dependent variations in leaf respiration in a dry-land, low  
708 productivity Mediterranean forest: The importance of acclimation in both high-light and  
709 shaded habitats, *Funct. Ecol.*, 22(1), 172–184, doi:10.1111/j.1365-2435.2007.01355.x, 2008.

710 Zolkos, S. G., Goetz, S. J. and Dubayah, R.: A meta-analysis of terrestrial aboveground  
711 biomass estimation using lidar remote sensing, *Remote Sens. Environ.*, 128, 289–298,  
712 doi:10.1016/j.rse.2012.10.017, 2013.

713

714

Formatted: Spanish (Spain)

715 **Table 1:** Specifications for the lidar surveys undertaken at Alto Tajo (Spain) in 2006 and  
716 2011.

	2006	2011
Lidar sensor	Optech-ALTM3033	Leica ALS050
Wavelength (nm)	1064	1064
Beam divergence (mrad)	0.20	0.22
Vertical discrimination (m)		2.8
Detection system	Two return	Four return
Date of deployment	16 May 2006	21 May 2011
Pulse rate frequency (MHz)	33.33	67.2–74.4
FoV (degrees)	12	40
Scan frequency (Hz)	42.4	35.8–40.0
Point density (m <sup>-2</sup> )	0.5	2
Number of flight lines	3(N–W)	4 (E–W) + 3(N–W)
Altitude (m) <b>a.s.l.</b>	2063–2073	2097–2140

717

718

Formatted: Not Highlight

719 **Table 2:** Comparison of the lidar modelling of above-ground biomass (AGB) and biomass  
720 change (AGB change) with forest inventory and tree-ring data: values given are mean (and  
721 standard deviation in parentheses).

	<b>Lidar data</b>	<b>Forest inventory data</b>	<b>Tree-ring data</b>
AGB (Mg/ha)	41.80 ( $\pm$ 25.68)	42.8 ( $\pm$ 52.7)	-
AGB change (Mg/ha/yr)	1.22 ( $\pm$ 1.92)	1.19 ( $\pm$ 1.17)	1.13( $\pm$ 0. 54)
Sample size	9136 grid cells	66 plots	13 plots

722

723

724 **Table 3:** Average above-ground biomass (AGB) and carbon sequestration potential over a 100  
725 year period for the four forest fire scenarios (no fire and at annual fire probability of occurrence  
726 of  $p=0.002$ ,  $0.004$  and  $0.01$ ), scaled up to the regional level (181,000 ha of mixed forest in  
727 Castilla la Mancha) for carbon and carbon-dioxide equivalence.

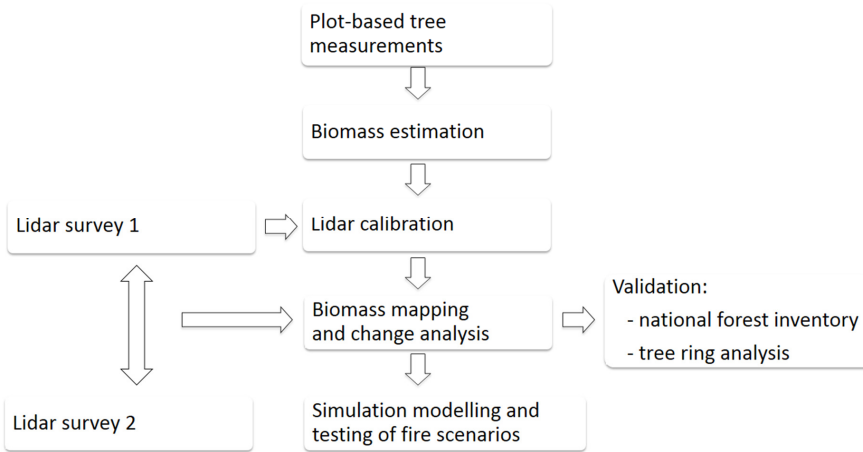
<b>Fire scenario</b>	<b>AGB (Mg/ha)</b>	<b>Carbon sequestration potential (Mg/ha)</b>	<b>Regional carbon (Kt)</b>	<b>Regional CO<sub>2</sub> equivalent (Kt)</b>
No fire	124.9	58.7	10.6	39.0
$P=0.002$	111.6	52.4	9.5	34.8
$P=0.004$	101.9	47.9	8.7	31.8
$P=0.01$	77.7	36.5	6.6	24.3

728

729

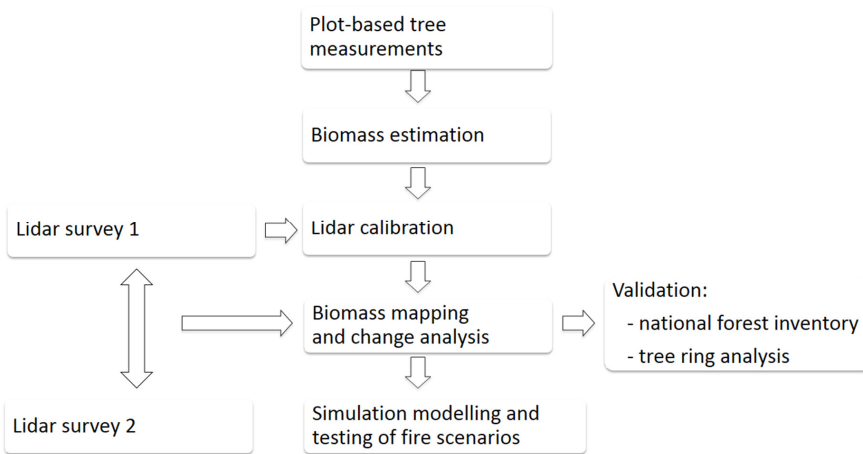


730  
731  
732



Formatted: Font: Times New Roman, 12 pt

733



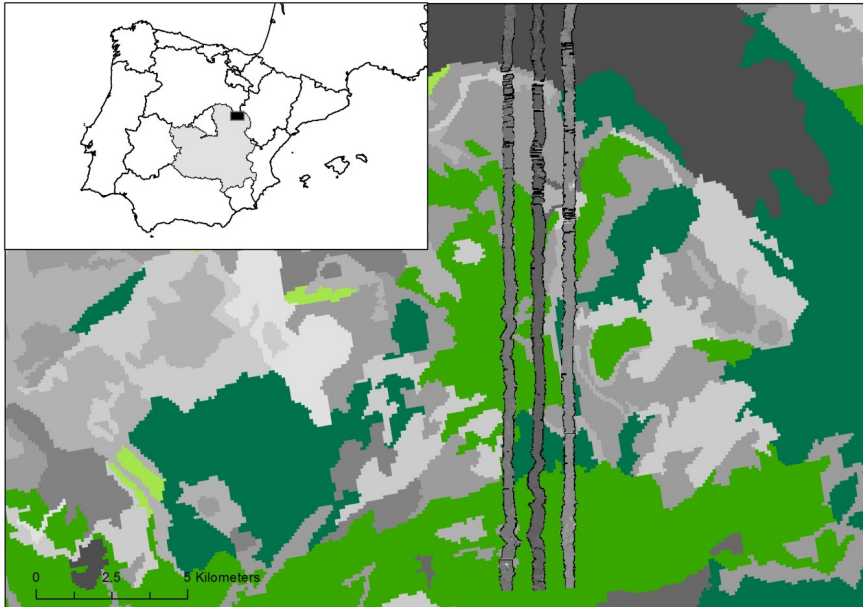
Formatted: Font: Times New Roman, 12 pt

734  
735

736 **Figure 1:** Methodological approach.

737

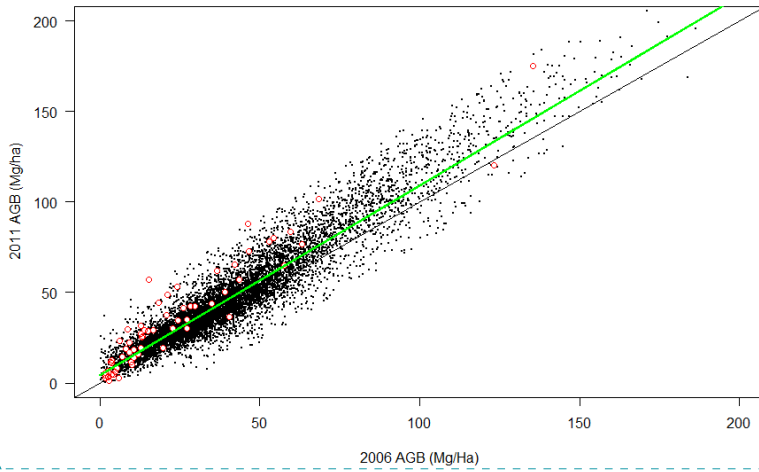
738



739

740 **Figure 2:** Study area. Shown in lighter green, mixed forest, and darker green, coniferous  
741 forest. Other land covers (including agricultural) in shades of grey, with darkest grey  
742 indicating an area burned by forest fire in 2005 and excluded from these analyses. The three  
743 north-south parallel strips show the lidar survey coverage.

744



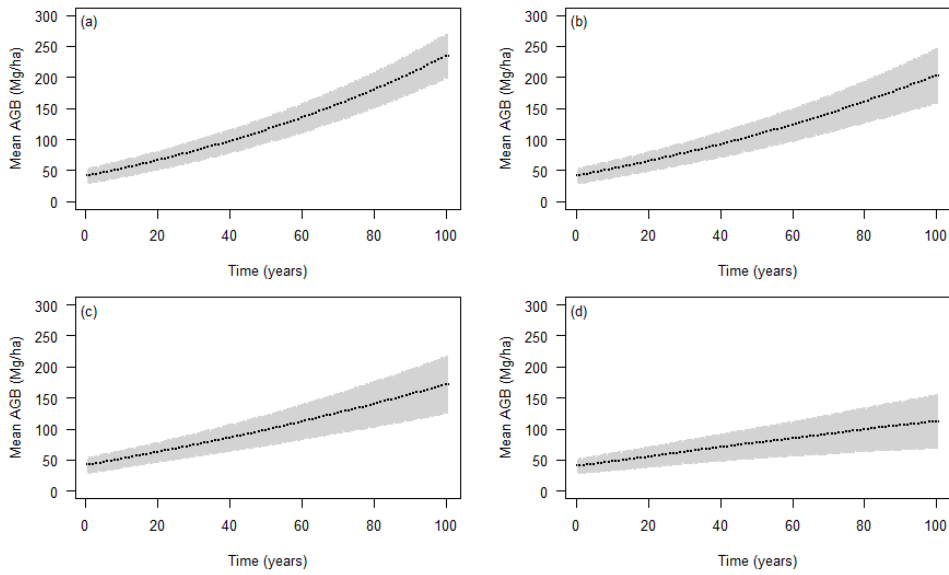
745

746

747 **Figure 3:** Scatterplot of above-ground biomass (AGB) estimates for 2006 and 2011: lidar  
748 (black dots), Spanish Forest Inventory (red bordered circles), with one-to-one line (black) and  
749 fitted model (green).

750

Formatted: Font: Times New Roman, 12 pt



751 **Figure 4:** Simulation model results for AGB over a 100 year period without fire (a) and at  
 752 annual fire probability of occurrence of  $p=0.002$  (b),  $0.004$  (c) and  $0.01$  (d). Figures show  
 753 mean (black line) and 95% confidence intervals (grey shading).

754

755

756

**Formatted:** Font: Bold

757 **Appendix A**

758 Allometric equations used in the estimation of tree biomass from height and stem diameter  
759 measurements

760 ~~(Ruiz Peinado, del Rio, & Montero, 2011; Ruiz Peinado, Montero, & del Rio, 2012)~~

761 (Ruiz-Peinado et al., 2011, 2012)

762 *Pinus nigra* Arn.

763	Stem $W_s =$	$0.0403 \cdot d \cdot 1.838 \cdot h^{0.945}$
764	Thick branches	If $d \leq 32.5$ cm then $Z = 0$ ; If $d > 32.5$ cm then $Z = 1$ ;
765	$W_{b7} =$	$[0.228 \cdot (d-32.5)^2] \cdot Z$
766	Medium branches $W_{b2-7} =$	$0.0521 \cdot d^2$
767	Thin branches + needles $W_{b2+n} =$	$0.0720 \cdot d^2$
768	Roots $W_r =$	$0.0189 \cdot d^{2.445}$

Formatted: Portuguese (Portugal)

769 *Pinus sylvestris* L.

770	Stem $W_s =$	$0.0154 \cdot d^2 \cdot h$
771	Thick branches	If $d \leq 37.5$ cm then $Z = 0$ ; If $d > 37.5$ cm then $Z = 1$ ;
772	$W_{b7} =$	$[0.540 \cdot (d-37.5)^2 - 0.0119 \cdot (d-37.5)^2 \cdot h] \cdot Z$
773	Medium branches $W_{b2-7} =$	$0.0295 \cdot d^{2.742} \cdot h^{-0.899}$
774	Thin branches + needles $W_{b2+n} =$	$0.530 \cdot d^{2.199} \cdot h^{-1.153}$
775	Roots	$W_r = 0.130 \cdot d^2$

776 *Juniperus thurifera* L. (applied for all *Juniperus*)

777	Stem $W_s =$	$0.0132 \cdot d^2 \cdot h + 0.217 \cdot d \cdot h$
778	Thick branches	If $d \leq 22.5$ cm then $Z = 0$ ; If $d > 22.5$ cm then $Z = 1$ ;
779	$W_{b7} =$	$[0.107 \cdot (d-22.5)^2] \cdot Z$
780	Medium branches $W_{b2-7} =$	$0.00792 \cdot d^2 \cdot h$
781	Thin branches + needles $W_{b2+n} =$	$0.273 \cdot d \cdot h$
782	Roots $W_r =$	$0.0767 \cdot d^2$

783 *Quercus faginea*

784	Stem $W_s =$	$0.154 \cdot d^2$
785	Thick branches $W_{b7} =$	$0.0861 \cdot d^2$
786	Medium branches $W_{b2-7} =$	$0.127 \cdot d^2 - 0.00598 \cdot d^2 \cdot h$
787	Thin branches + leaves $W_{b2+l} =$	$0.0726 \cdot d^2 - 0.00275 \cdot d^2 \cdot h$
788	Roots $W_r =$	$0.169 \cdot d^2$

789 *Quercus ilex*

790	Stem $W_s =$	$0.143 \cdot d^2$
791	Thick branches	If $d \leq 12.5$ cm then $Z = 0$ ; If $d > 12.5$ cm then $Z = 1$ ;
792	$W_{b7} =$	$[0.0684 \cdot (d - 12.5)^2 \cdot h] \cdot Z$
793	Medium branches $W_{b2-7} =$	$0.0898 \cdot d^2$
794	Thin branches + leaves $W_{b2+l} =$	$0.0824 \cdot d^2$
795	Roots $W_r =$	$0.254 \cdot d^2$

796

797 *Notes:*

798  $W_s$ : Biomass weight of the stem fraction (kg);

799  $W_{b7}$ : Biomass weight of the thick branches fraction (diameter larger than 7 cm) (kg);

800  $W_{b2-7}$ : Biomass weight of medium branches fraction (diameter between 2 and 7 cm) (kg);

801  $W_{b2+l}$ : Biomass weight of thin branches fraction (diameter smaller than 2 cm) with leaves (kg);

802  $W_r$ : Biomass weight of the belowground fraction (kg);

803 *d*: diameter at breast height (cm);  
804 *h*: tree height (m);

